Printed in U.S.A.

Paper No.
73-DET-103

an ASME publication

J. W. LUND

Department of Machine Design,
The Technical University of Denmark,
Lyngby, Denmark

Stability and Damped Critical Speeds of a Flexible Rotor in Fluid-Film Bearings

A method is described for calculating the threshold speed of instability and the damped critical speeds of a general flexible rotor in fluid-film journal bearings. It is analogous to the Myklestad-Prohl method for calculating critical speeds and is readily programmed for numerical computation. The rotor model can simulate any practical shaft geometry and support configuration. The bearings are represented by their linearized dynamic properties, also known as the stiffness and damping coefficients of the bearing, and the calculation includes hysteretic internal damping in the shaft and destabilizing aerodynamic forces. To demonstrate the application of the method, results are shown for an industrial, multistage compressor.

Introduction

An important part of the standard design procedure for a rotor is the calculation of its critical speeds. Furthermore, in recent years methods have become available to investigate whether a rotor may experience instability because of the journal bearings, internal shaft damping, aerodynamic excitation, or from other sources. This paper describes a computational method to perform both types of calculations simultaneously.

The critical speeds of a rotor are frequently computed assuming the bearings to act as rigid supports. It is, however, well known that bearings have flexibility which inherently lower the critical speeds but, at least with oil-lubricated bearings, shop tests normally confirm the results of the rigid bearing calculations. The primary cause of this apparent discrepancy is the substantial bearing damping which acts in series with the shaft flexibility, thereby contributing to a stiffening of the bearing. The effect, which depends on the ratio between shaft and bearing stiffnesses, is included by the present method. A conventional critical speed calculation finds, by its very nature, the undamped resonant frequencies of the rotor. In the general case, as considered presently, it is the damped natural frequencies which are to be determined. Thus, denoting any rotor amplitude as x, a free vibration can be expressed as

$$x = |x| \cdot e^{\lambda t} \cos(\omega t + \psi) = \mathrm{Re}\{(x_c + ix_s)e^{st}\} \qquad (1)$$

where $|x|$ is the amplitude, ψ is an appropriate phase angle, ω is the damped natural frequency, λ is the corresponding damping exponent, and s is the complex frequency

$$s = \lambda + i\omega \qquad (2)$$

Usually λ is negative such that the vibration dies out exponentially with time. Should λ, however, become positive, the amplitude will increase with time and the rotor is unstable. Thus both the critical speeds of the rotor and its threshold of instability are determined from a calculation of those values of s, also called the eigenvalues, at which the system can perform damped free vibrations.

Damped Natural Frequencies and Their Modes

To study the nature of the eigenvalues, an analysis has been performed for a uniform shaft supported at the ends in damped bearings. The analysis is given in the Appendix.

Numerical results have been obtained for a uniform shaft with a length of 50 in., a diameter of 4 in., a Young's modulus of $3 \cdot 10^7$ psi and a weight density of 0.283 lb/in^3. For simplicity the shaft is treated as a uniform beam, disregarding shear deformations, rotary inertia, and gyroscopic effects. It is supported at the ends in identical bearings, and with rigid bearings the natural frequencies are 127.11 cps, 508.44 cps, 1143.99 cps, 2033.76 cps, etc.

When the rigid supports are replaced by resilient bearings, represented by a spring coefficient and a damping coefficient, the results are shown in Figs. 1 and 2 for bearing stiffness values of 20,000 and 60,000 lb in., respectively. The abscissa is the damping exponent λ sec^{-1}, equation (1); the ordinate is the corresponding damped natural frequency ω in cps, and the values on the curves give the bearing damping coefficient in lb·sec/in.

Contributed by the Vibration and Sound Committee of the Design Engineering Division of The American Society of Mechanical Engineers for presentation at the Design Engineering Technical Conference Cincinnati, Ohio, September 9–12, 1973. Manuscript received at ASME Headquarters, June 6, 1973. Paper No. 73-Det-103.

Copies will be available until June, 1974.

Using as an example a bearing damping coefficient of 500 lb·sec/in., Fig. 1 shows that the two lowest modes are critically damped. The third shows up at a frequency slightly below the first rigid bearing critical speed; the fourth mode comes in just above the second rigid bearing critical, and similarly for the higher modes. Hence, the critical speeds observed in a test would agree well with the results obtained on the basis of rigid bearings, but the mode number differs from the critical speed number.

Stiffening up the bearing as shown in Fig. 2 results in the second and third mode being critically damped instead of the first and the second, as in Fig. 1. In this case, the first critical speed corresponds with the first mode and, as before, the frequency is just below the value computed with rigid bearings. For the second and the higher critical speeds, the situation is the same as previously stated.

In the analysis, in the Appendix, it is shown that a maximum of two modes can be critically damped for this simple shaft-bearing system. As discussed later, this seems to be generally true, at alest for systems that are reasonably close to being symmetric.

In an actual rotor, the bearings usually have different stiffness and damping properties in, say, the vertical and horizontal directions. Thus each mode will split up into two, one mode corresponding to the minimum bearing stiffness and one mode to the maximum bearing stiffness. In the absence of any damping and with no interference from other modes, it is readily seen that the rotor will be in a state of backward precession between the two modal frequencies and, although the presence of damping and the overlapping of modes complicate the picture, it is normally found that one mode has predominantly forward precession while the other mode is predominantly in backward precession. This is further amplified by the gyroscopic moments in the rotor. As an example, Fig. 3 shows the damped natural frequencies of the same uniform shaft as just considered but now supported in plain cylindrical bearings. The journal diameter is 4 in., the radial clearance is 0.002 in., the bearing length is 1 in., the oil viscosity is 6.9 centipoise, and the bearing load, equal to half the shaft

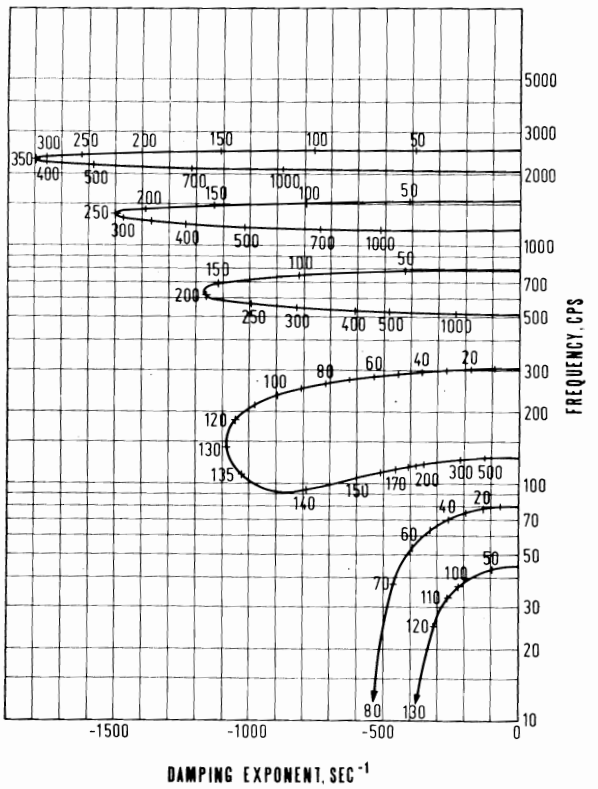

Fig. 1 Damped natural frequencies of uniform shaft in flexible bearings. Bearing stiffness = 20,000 lb/in. Bearing damping coefficient given in lb. sec/in. by values on curves.

Nomenclature

A = cross-sectional area of shaft, in.^{2}

$\underline{\underline{B}}$ = 4 × 4 matrix of support damping coefficients

$B_{xx}, B_{xy}, B_{x\theta}, \ldots$ = support damping coefficients with units: lb·sec/in., lb·sec/rad, lb-in.·sec/in. or lb-in.·sec/rad; first index is direction of reaction; second index is amplitude direction

$\underline{D}$ = 4 × 4 complex matrix of residual bending moments and shear forces

E = Young's modulus, psi

f_0, f_l = bearing reactions at shaft ends, lb

G = shear modulus, psi

I = cross-sectional transverse moment of inertia of shaft, in.^{4}

i = imaginary unit

J_{Pn} = polar mass moment of inertia at station no. n, lb-in.·sec^2

J_{Tn} = transverse mass moment of inertia at station n, lb-in.·sec^2

$\underline{\underline{K}}$ = 4 × 4 matrix of support stiffness coefficients

$K_{xx}, K_{xy}, K_{x\theta}, \ldots$ = support stiffness coefficients with units: lb/in., lb/rad, lb-in/in. or lb-in/rad

l = shaft length, in.

M_x, M_y = bending moments, lb-in.

m_n = mass at station no. n, lb·sec^2/in.

N_n = modal norm

s = $\lambda + i\omega$, the complex frequency, rad/sec

t = time, sec

V_x, V_y = shear forces, lb

X_n = modal function no. n for a free-free beam

x, y = radial shaft displacements, in.

z = coordinate along axis of shaft, in.

Z_r = shaft impedance at the ends of a free-free beam, lb/in.

α = cross-sectional shape factor for shear deformation of shaft ($\alpha \simeq 0.75$ for circular cross section)

γ = phase angle between stress and strain in hysteretic damping

Δ = det(D), residual determinant

δ = $-2\pi\lambda/\omega$, logarithmic decrement of damped shaft vibrations

ϵ = logarithmic decrement of internal shaft damping, divided by π

θ, ϕ = angular shaft displacements, rad

λ = damping exponent of free vibrations of shaft, sec^{-1}

ρ = mass density of shaft, lb·sec^2/in.^{4}

Ω = angular speed of shaft, rad/sec

ω = frequency of free vibrations of shaft, rad/sec

ω_0 = fundamental resonant frequency of simply supported beam, rad/sec

Indexes

x = x-direction; in the x-z-plane

y = y-direction; in the y-z-plane

n = rotor station number

n = in Appendix, the mode number

$0, l$ = at the shaft ends

$\cdot$ = differentiation with respect to time

weight, is 88.9 lb. For this type of bearing there are four stiffness coefficients and four damping coefficients which are functions of the bearing Sommerfeld number and, therefore, depend on the rotor speed.

The results are obtained from the analysis in the Appendix. With the rotor speed as abscissa and the damped natural frequency as ordinate, a number of the modes are shown in Fig. 3. The parameter values on the curves give the logarithmic decrement instead of the damping exponent

$$\text{logarithmic decrement:} \quad \delta = -\frac{2\pi\lambda}{\omega} = \frac{-\lambda}{\text{frequency, cps}} \qquad (3)$$

When the value of δ exceeds 1, that particular mode is well damped. As just discussed, each rotor mode actually consists of two modes, one with forward precession and one with backward precession, identified by the letters "F" and "B," respectively, on the curves. In addition, "E" identifies even modes where the end amplitudes are in phase, and "O" are for the odd modes where the end amplitudes are out of phase. The first rotor mode is even, the second is odd, and so on. In Fig. 3 the backward precessional modes of the first and second rotor modes are critically damped and are, therefore, not shown.

On the figure is a curve for the synchronous frequency at which any mass unbalance excites the rotor. The intersections between this curve and any of the modal frequency curves give the damped critical speeds of the rotor. It is seen that the first and second modes never become excited while the third mode is synchronous at approximately 125 cps or 7500 rpm. This would in practice be recognized as the first critical speed of the rotor in close agreement with the 127 cps calculated for rigid bearing supports. A similar agreement is seen between the fourth mode and the second rigid bearing critical speed of 508 cps but this speed cannot be reached because the rotor becomes unstable in oilwhip at 9160 rpm.

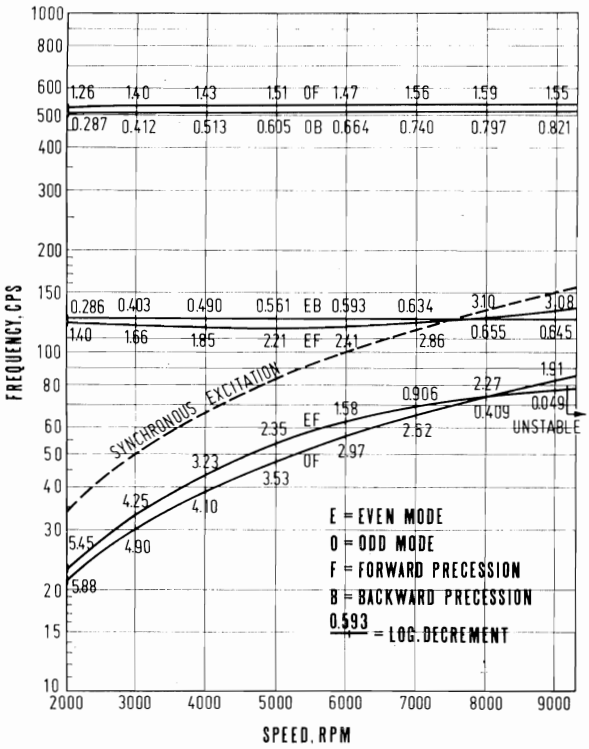

Fig. 3 Damped natural frequencies of uniform shaft in plain cylindrical journal bearings (diameter = 4 in., length = 1 in., radial clearance = 0.002 in., load = 88.9 lb, oil viscosity = 6.9 centipoise).

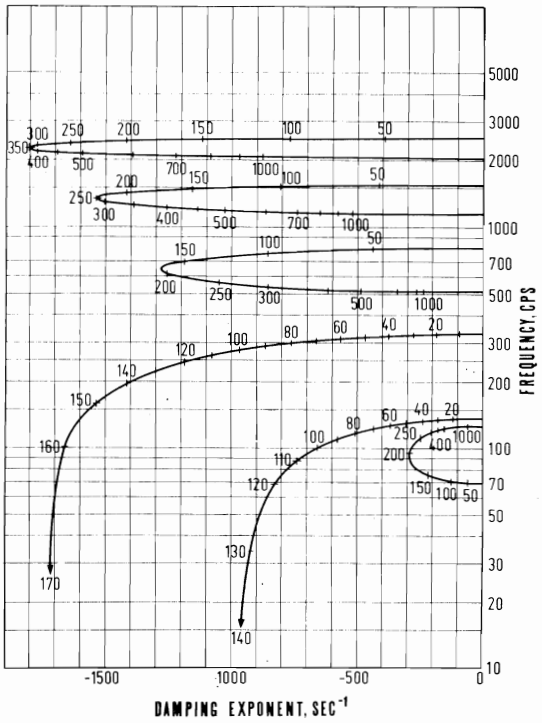

Fig. 2 Damped natural frequencies of uniform shaft in flexible bearings. Bearing stiffness = 60,000 lb/in. Bearing damping coefficient given in lb. sec/in. by values on curves.

The whirl frequency at onset of instability is 78 cps, very close to one-half of the rotational frequency, as would be expected. The rotor whirls in its first mode (with forward precession) but this mode is not the first critical speed, as just discussed. The threshold of instability is, therefore, not at twice the first critical speed, as is otherwise an accepted rule of thumb although, as seen, it equals twice the frequency of the first mode. This example demonstrates that even though a rigid bearing critical speed calculation may successfully predict unbalance response peaks, the same results cannot necessarily be used to predict the speed at which oilwhip is encountered.

Analysis

For the purpose of computing the damped, natural frequencies (eigenvalues), a rotor-bearing system can be represented mathematically by a stiffness matrix, a damping matrix, and an inertia matrix from which the eigenvalue problem can be formulated. The dimension of the resulting matrix, however, equals 8 times the number of mass stations in the system which, in a practical rotor calculation, may mean a matrix size of, for example, 240 by 240. Further complications arise from the matrix being unsymmetric, requiring special modifications in the available standard methods for calculating eigenvalues. For these reasons an alternative method is desirable and, in the following, a computational procedure is developed, based on the widely used method by Myklestad and Prohl [1, 2].[1]

[1] Numbers in brackets designate References at end of paper.

The rotor is supported in fluid-film bearings whose dynamic properties are given through a set of stiffness and damping coefficients. The bearing reaction, for example, in the x-direction can be expressed as

$$\text{reaction in } x\text{-direction} = -K_{xx}x - K_{xy}y - K_{x\theta}\theta - K_{x\phi}\phi - B_{xx}\dot{x} - B_{xy}\dot{y} - B_{x\theta}\dot{\theta} - B_{x\phi}\dot{\phi} \qquad (4)$$

and similarly for the reactions in the y, θ, and ϕ-directions ("dot" indicates differentiation with respect to time). There are 32 coefficients in all which can be arranged in a stiffness matrix $\underline{\underline{K}}$ and a damping matrix $\underline{\underline{B}}$, respectively.

The coefficients are obtained from the lubrication equation (Reynold's equation) as the gradients of the hydrodynamic forces. A numerical scheme for such a calculation can be found in [14]. For conventional journal bearings, only the radial coefficients, namely, K_{xx}, K_{xy}, K_{yx}, K_{yy}, and the four corresponding damping coefficients, are of importance. On the other hand, for very short rotors or at higher-order shaft modes the angular coefficients may also be of significance.

Equation (4) also describes certain aerodynamic forces in turbomachinery. In axial flow compressors and turbines, a radial displacement of the wheel in a stage sets up a transverse force, proportional to the displacement. With the notation of equation (4) the coefficient of proportionality becomes [25]

$$K_{xy} = -K_{yx} = \beta \frac{T}{2rh} \tag{5}$$

where T is the stage torque, r is the pitch radius, h is the vane height, and β is a dimensionless parameter, giving the gradient of the normalized stage efficiency curve as a function of the clearance-to-vane height ratio (β is of the order of 1). The remaining stiffness and damping coefficients are equal to zero.

As in the conventional Myklestad-Prohl method, the rotor is represented in the calculations by a series of lumped masses, called stations, which are connected by uniform shaft sections. Stations are provided at the two free ends of the rotor, at the bearing center lines, at places where heavy components are mounted on the shaft such as wheels, impellers, or thrust collars, and at locations where the shaft diameter changes significantly. The shaft section between two stations can then be assumed to be uniform and its mass may be treated either as being distributed [8], or it may be lumped at the ends of the section at the stations. When the latter procedure is chosen, as in the present analysis, there must be a sufficient number of stations to represent adequately the highest mode in the frequency range of interest. The radial amplitudes at station number n are x_n and y_n, and the corresponding angular amplitudes are θ_n and ϕ_n. For free vibrations of the form given in equation (1), these quantities become complex and the equations of motion for station n are (see Fig. 4)

$$\begin{Bmatrix} -V'_{xn} \\ -V'_{yn} \\ M'_{xn} \\ M'_{yn} \end{Bmatrix} = \begin{Bmatrix} -V_{xn} \\ -V_{yn} \\ M_{xn} \\ M_{yn} \end{Bmatrix} + \begin{Bmatrix} s^2 m_n x_n \\ s^2 m_n y_n \\ s^2 J_{Tn}\theta_n + s\Omega J_{Pn}\phi_n \\ s^2 J_{Tn}\phi_n - s\Omega J_{Pn}\theta_n \end{Bmatrix} + (\underline{\underline{K}} + s\underline{\underline{B}})_n \begin{Bmatrix} x_n \\ y_n \\ \theta_n \\ \phi_n \end{Bmatrix} \tag{6}$$

In the further analysis, the derivatives of the variables with respect to s are also required

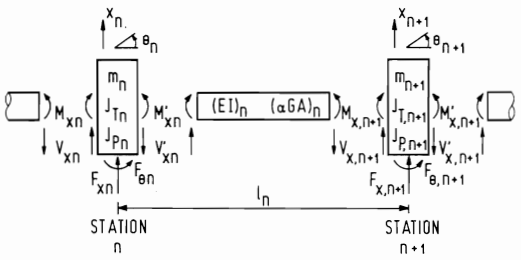

Fig. 4 Sign convention for radial displacement, angular displacement, bending moment, and shear force

$$\begin{Bmatrix} -\frac{dV'_{xn}}{ds} \\ -\frac{dV'_{yn}}{ds} \\ \frac{dM'_{xn}}{ds} \\ \frac{dM'_{yn}}{ds} \end{Bmatrix} = \begin{Bmatrix} -\frac{dV_{xn}}{ds} \\ -\frac{dV_{yn}}{ds} \\ \frac{dM_{xn}}{ds} \\ \frac{dM_{yn}}{ds} \end{Bmatrix} + \begin{Bmatrix} s^2 m_n \frac{dx_n}{ds} \\ s^2 m_n \frac{dy_n}{ds} \\ s^2 J_{Tn}\frac{d\theta_n}{ds} + s\Omega J_{Pn}\frac{d\phi_n}{ds} \\ s^2 J_{Tn}\frac{d\phi_n}{ds} - s\Omega J_{Pn}\frac{d\theta_n}{ds} \end{Bmatrix}$$

$$+ (\underline{\underline{K}} + s\underline{\underline{B}})_n \begin{Bmatrix} \frac{dx_n}{ds} \\ \frac{dy_n}{ds} \\ \frac{d\theta_n}{ds} \\ \frac{d\phi_n}{ds} \end{Bmatrix} + \begin{Bmatrix} 2sm_n x_n \\ 2sm_n y_n \\ 2sJ_{Tn}\theta_n + \Omega J_{Pn}\phi_n \\ 2sJ_{Tn}\phi_n - \Omega J_{Pn}\theta_n \end{Bmatrix} + \underline{\underline{B}} \cdot \begin{Bmatrix} x_n \\ y_n \\ \theta_n \\ \phi_n \end{Bmatrix} \tag{7}$$

The shaft sections are assumed to have internal material dumping of hysteretic type where the dissipated energy is independent of frequency. The stress leads the corresponding strain by an angle γ which is a material property. The hysteresis loop in the stress-strain plane is an ellipse whose area, proportional to $\sin\gamma$, gives a measure of the dissipated energy such that

$$\sin\gamma \simeq \frac{\epsilon}{\sqrt{1+\epsilon^2}}$$

where $\pi\epsilon$ is equal to the logarithmic decrement for the shaft. The relationship between bending strain and bending stress becomes [3]

$$\begin{aligned} \frac{d\theta}{dz} &= \frac{1}{EI} M_x \cos\gamma - \frac{1}{EI} M_y \sin\gamma \\ \frac{d\phi}{dz} &= \frac{1}{EI} M_x \sin\gamma + \frac{1}{EI} M_y \cos\gamma \end{aligned} \tag{8}$$

or

$$\begin{aligned} \frac{d\theta}{dz} &= \frac{1}{EI\sqrt{1+\epsilon^2}} \cdot (M_x - \epsilon M_y) \\ \frac{d\phi}{dz} &= \frac{1}{EI\sqrt{1+\epsilon^2}} \cdot (M_y + \epsilon M_x) \end{aligned} \tag{9}$$

When the whirl orbit is circular, this effect may be accounted for by making the E-modulus complex [30].

The adopted form of internal shaft damping is representative of material hysteretic damping and dry friction. It is independent of frequency. In much rotor dynamic analysis the internal damping is considered in another form, namely, as frequency-dependent, viscous damping which is proportional to the entrained strain velocity [4–6, 9]. In that case the shaft equations become

$$\begin{aligned} \frac{1}{EI}\cdot M_x &= \frac{d\theta}{dz} + \epsilon\cdot\left(\frac{d\dot{\theta}}{dz} + \Omega\frac{d\phi}{dz}\right) = (1+s\epsilon)\frac{d\theta}{dz} + \Omega\epsilon\frac{d\phi}{dz} \\ \frac{1}{EI}\cdot M_y &= \frac{d\phi}{dz} + \epsilon\cdot\left(\frac{d\dot{\phi}}{dz} - \Omega\frac{d\theta}{dz}\right) = (1+s\epsilon)\frac{d\phi}{dz} - \Omega\epsilon\frac{d\theta}{dz} \end{aligned} \tag{10}$$

where $\pi\epsilon$ is equal to the logarithmic decrement of the viscous damping. These equations take the place of equation (9) when viscous damping is considered.

Whereas the hysteretic form of damping always is destabilizing, internal viscous damping does not begin to act destabilizing until the rotor reaches a certain speed which, in the special case of undamped, isotropic supports, equals the first critical speed.

The hysteretic form of internal damping, used in the following, is believed to be a more valid representation for a practical rotor than viscous damping, but the subject matter is not well understood. From the conventional beam equations, modified by equation (9), the transfer equations for a shaft section become (see Fig. 4)

$$x_{n+1} = x_n + l_n\theta_n + \frac{1}{(EI)_n\sqrt{1+\epsilon^2}}\cdot\left[\frac{l_n^2}{2}(M'_{xn} - \epsilon M'_{yn}) + \left(\frac{l_n^3}{6} - \frac{(lEI)_n}{(\alpha GA)_n}\right)(V'_{xn} + \epsilon V'_{yn})\right]$$

$$y_{n+1} = y_n + l_n\phi_n + \frac{1}{(EI)_n\sqrt{1+\epsilon^2}}\cdot\left[\frac{l_n^2}{2}(M'_{yn} + \epsilon M'_{xn}) + \left(\frac{l_n^3}{6} - \frac{(lEI)_n}{(\alpha GA)_n}\right)(V'_{yn} + \epsilon V'_{xn})\right]$$

$$\theta_{n+1} = \theta_n + \frac{1}{(EI)_n\sqrt{1+\epsilon^2}}\cdot\left[l_n(M'_{xn} - \epsilon M'_{yn}) + \frac{l_n^2}{2}(V'_{xn} - \epsilon V'_{yn})\right] \quad (11)$$

$$\phi_{n+1} = \phi_n + \frac{1}{(EI)_n\sqrt{1+\epsilon^2}}\cdot\left[l_n(M'_{yn} + \epsilon M'_{xn}) + \frac{l_n^2}{2}(V'_{yn} + \epsilon V'_{xn})\right]$$

$$M_{x,n+1} = M'_{xn} + l_nV'_{xn}$$

$$M_{y,n+1} = M'_{yn} + l_nV'_{yn}$$

$$V_{x,n+1} = V'_{xn}$$

$$V_{y,n+1} = V'_{yn}$$

The equations for the derivatives of the variables with respect to s are obviously identical to the foregoing equations.

The two ends of the rotor are assumed to be free. Thus, with a total of N rotor stations, the boundary conditions are

$$M_{x1} = M_{y1} = V_{x1} = V_{y1} = 0 \quad (12)$$

$$M'_{xN} = M'_{yN} = V'_{xN} = V'_{yN} = 0 \quad (13)$$

The calculation procedure is analogous to the one used in the Myklestad-Prohl method. Thus, with an assumed value of s, a total of 4 calculations is performed. In the first calculation, $x_1 = 1$ while $y_1 = \theta_1 = \phi_1 = 0$. In the second calculation, $y_1 = 1$ while $x_1 = \theta_1 = \phi_1 = 0$, and similarly, in the third and fourth calculations, with $\theta_1 = 1$ and $\phi_1 = 1$, respectively. With the starting values being independent of the value of s, the starting values of the derivatives are zero

$$\frac{dx_1}{ds} = \frac{dy_1}{ds} = \frac{d\theta_1}{ds} = \frac{d\phi_1}{ds} = \frac{dM_{x1}}{ds} = \frac{dM_{y1}}{ds} = \frac{dV_{x1}}{ds} = \frac{dV_{y1}}{ds} = 0 \quad (14)$$

Thus, in each of the four calculations, the values of the variables and their derivatives are known at the first rotor station. Thereafter repetitive use of equations (6), (7), and (11) makes it possible to go through the shaft station by station until the last station, number N, is reached. The results of the four calculations may be combined in a matrix equation

$$\begin{Bmatrix} M'_{xN} \\ M'_{yN} \\ V'_{xN} \\ V'_{yN} \end{Bmatrix} = \underline{\underline{D}} \begin{Bmatrix} x_1 \\ y_1 \\ \theta_1 \\ \phi_1 \end{Bmatrix} \quad (15)$$

where $\underline{\underline{D}}$ is a 4×4 matrix whose first column has as its elements the values of M'_{xN}, M'_{yN}, V'_{xN}, and V'_{yN} obtained from the first rotor calculation with $x_1 = 1$, and similarly for columns 2, 3, and 4.

To satisfy the boundary condition of equation (13), equation (15) must be equal to zero. The values of s for which this is satisfied and where the solution is not trivial, are those values which make the determinant of $\underline{\underline{D}}$ equal to zero

$$\Delta = \det(\underline{\underline{D}}) = 0 \quad (16)$$

Assume that for some value $s = s_0$, the corresponding, computed determinant is $\Delta = \Delta_0$. A first-order expansion yields

$$\Delta \simeq \Delta_0 + (s - s_0)\cdot\left(\frac{d\Delta}{ds}\right)_0 = 0 \quad (17)$$

Here $d\Delta/ds$ is the derivative of the determinant, calculated from

$$\frac{d\Delta}{ds} = \sum_{k=1}^{4}\Delta_k \quad (18)$$

where Δ_k is the determinant of the matrix $\underline{\underline{D}}$ where the elements in column k have been replaced by their derivatives as obtained from the four rotor calculations.

Equation (17) may be solved to yield a new estimate of the eigenvalue s

$$s = s_0 - \Delta_0\Big/\left(\frac{d\Delta}{ds}\right)_0 \quad (19)$$

To prevent the solution to converge toward an already obtained root, assume that a total of J roots has been found. As Δ is a polynomial in s, these roots can be eliminated by division whereby equation (17) is replaced by

$$\frac{\Delta_0}{\prod_{j=1}^{J}(s_0 - s_j)} + (s - s_0)\cdot\frac{d}{ds}\left(\frac{\Delta}{\prod_{j=1}^{J}(s - s_j)}\right)_0 = 0 \quad (20)$$

Hence equation (19) is replaced by

$$s = s_0 - \Delta_0\cdot\left[\left(\frac{d\Delta}{ds}\right)_0 - \Delta_0\sum_{j=1}^{J}\frac{1}{s_0 - s_j}\right]^{-1} \quad (21)$$

The roots occur either as real, separate roots, or in conjugate pairs. In the latter case, both roots should be eliminated in equation (21) when one of them has been found.

Starting with some estimated value of s equation (21) can be used repeatedly until the difference between two successive values becomes sufficiently small. In the calculations performed to obtain the results in the present paper, the accepted error is such that the eigenvalues are determined to an accuracy of 8 significant figures or better. Typically the number of iterations required for convergence is 5–10.

Calculations for an Industrial Compressor

To illustrate the application of the method, calculations are performed for an 8-stage centrifugal compressor, typical of machinery for chemical processing plants. The rotor weighs 1400 lb; it has an overall length of 103 in. and a bearing span of 80.7 in. Overhung at one end is the coupling while the thrust collar is overhung at the opposite end. The center of gravity is almost midway between the two identical bearings, which have a journal diameter of 5 in., a length of 1.5 in., and a radial clearance of 0.0035 in. The lubrication oil has a viscosity of 16.9 centipoise

at 120 deg F, decreasing to 8.1 centipoise at 160 deg F. The design speed of the machine is 8500 rpm.

A standard critical speed map for the rotor is shown in Fig. 5. It gives the undamped critical speeds as a function of bearing stiffness, assuming the two bearings to be identical. Such a diagram is normally prepared as a check of the design of the shaft and the bearings from a stiffness point of view.

Also shown on the diagram are the horizontal and vertical stiffnesses, labeled K_{min} and K_{maj}, respectively, for a 5 shoe tilting pad journal bearing as considered later in Figs. 7 and 8. Because of a small difference in load between the two bearings, there are two curves for each of the stiffnesses. Where the stiffness curves intersect the curves for the shaft are the undamped critical speeds of the rotor. It is seen that to reach the design speed of 8500 rpm (142 rps) the rotor passes through five critical speeds and is approaching a sixth critical speed. When damping is included, however, the situation changes significantly as shown later.

For later reference, Fig. 5 shows that with rigid bearings, the first four critical speeds are: 62.7 rps, 229 rps, 370 rps, and approximately 500 rps. To explore the possibility of supporting the rotor in plain cylindrical journal bearings with dimensions as just given, Fig. 6 shows the resulting damped natural frequency diagram. The same explanatory comments apply as given in connection with the discussion of Fig. 3. It is found that the rotor passes through four damped critical speeds, namely, the first mode with forward precession at 2748 rpm ($\delta = 0.857$), the first mode with backward precession at 3637 rpm ($\delta = 0.208$), the second mode with forward precession at 4180 rpm ($\delta = 2.27$), and the third mode with forward precession at 6840 rpm ($\delta = 1.12$). δ is the logarithmic decrement, defined in equation (3). The backward precessional modes of the second and third rotor modes are critically damped over the speed range and begin to appear at 8500-9000 rpm as seen in Fig. 6. Three of these four critical speeds are so well damped that they cannot be expected to amplify any unbalance vibrations significantly. Only the critical speed of 3637 rpm will be clearly observed by measurements and it will be identified as the first critical speed. At a frequency of 60.6 cps, it is seen to be quite close to the first rigid bearing critical of 62.7 cps.

Although they result in a satisfactory rotor performance from an unbalance response point of view, the plain cylindrical bearings cause the rotor to become unstable in oilwhip. In Fig. 6, the lowest mode (EF) loses its damping at 6100 rpm and is unstable beyond this threshold speed because of the negative logarithmic decrement. The whirl frequency is 49.2 cps, a little less than half the rotational frequency, and it is interesting to note that this frequency stays virtually constant with increasing speed past the onset of instability, a fact frequently observed in tests.

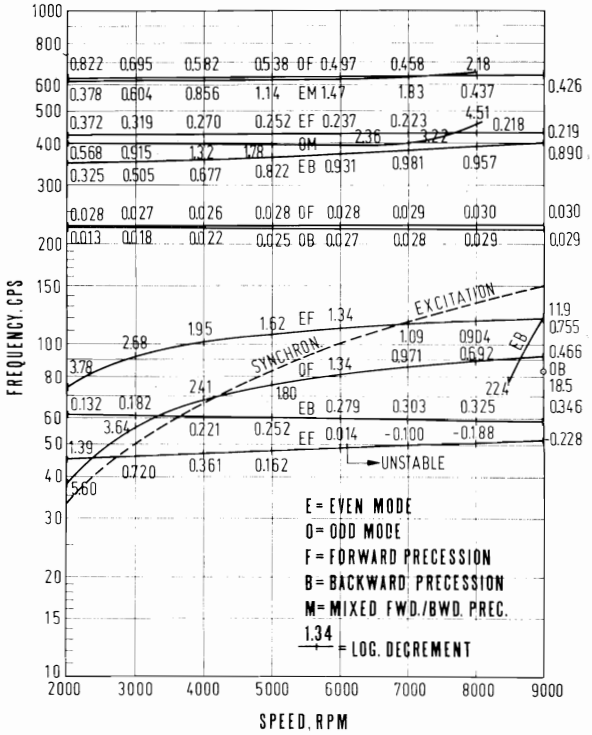

Fig. 6 Damped natural frequencies of 8 stage compressor in plain cylindrical journal bearings

Becoming unstable, the rotor whirls in the forward precessional mode of its first mode whereas it is the backward precessional mode which shows the largest unbalance response and, hence, will be identified as the first critical speed. The instability threshold speed, therefore, will be substantially less than twice the observed critical speed. With a threshold speed of 2400 rpm below the design speed of the rotor, it is difficult to devise means for modifying the plain cylindrical bearing that will insure stable operation at top speed. The simplest remedy is to employ tilting pad journal bearings.

The bearing dimensions are the same as used for the plain cylindrical bearings. The tilting pad bearing have five shoes of 60-deg arc length, centrally pivoted and set without preload. The bearing load vector passes through the pivot of the bottom pad.

The resulting diagram for the damped natural frequencies is shown in Fig. 7. As with the plain cylindrical bearing, the rotor passes through four critical speeds, but with the exception of the critical speed at 3550 rpm which now is the forward precessional

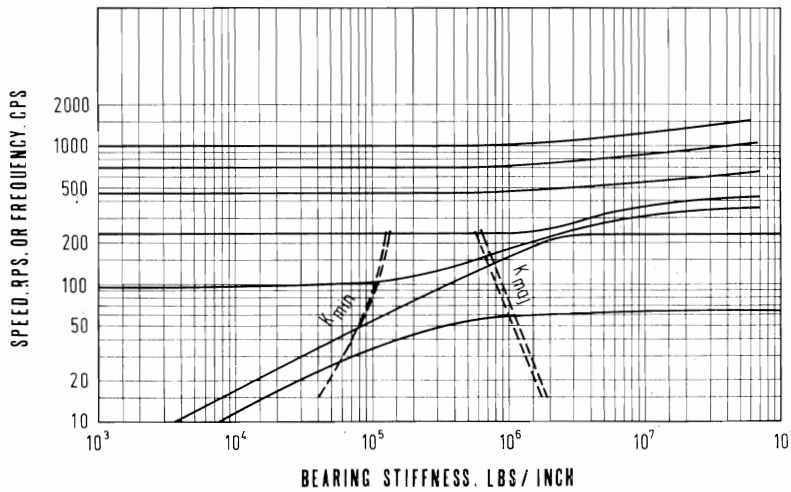

Fig. 5 Critical speed map for 8 stage centrifugal compressor

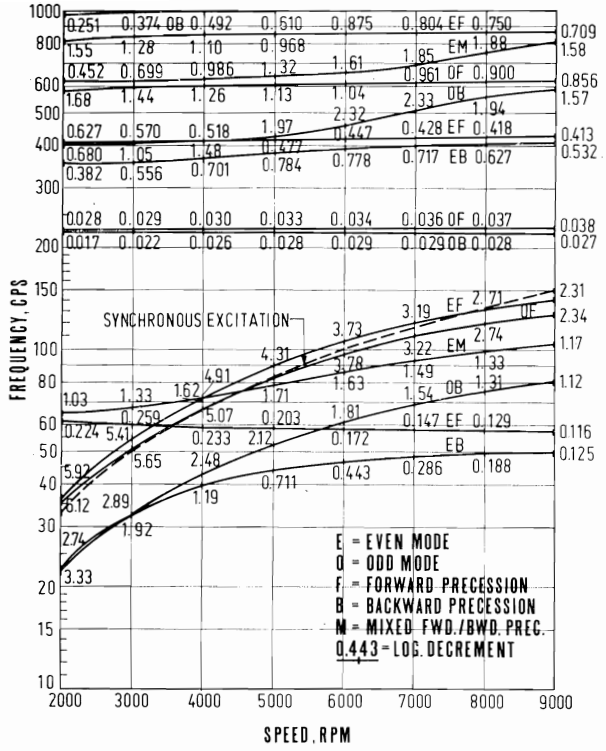

Fig. 7 Damped natural frequencies of 8 stage compressor in tilting pad journal bearings (5 pads)

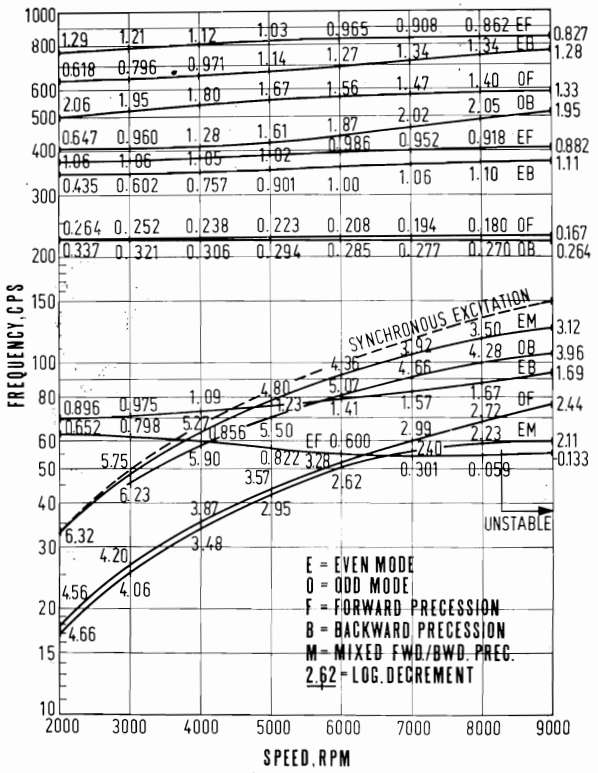

Fig. 8 Damped natural frequencies of 8 stage compressor in tilting pad journal bearings (5 pads) with oil seals

mode of the first rotor mode, the other critical speeds are strongly damped. Thus there is no sacrifice in unbalance response performance, and the rotor has been made inherently stable against oilwhip.

To check the margin of stability, calculations have been performed with destabilizing aerodynamic forces at each of the 8 impellers and with an internal hysteretic shaft damping of 0.1 in logarithmic decrement to simulate any dry friction in the shrink fits of the wheels and sleeves. No noticeable change is found in the modal damping exponents.

The rotor, however, is also provided with floating oilseals 6.8-in. inboard of each journal bearing. From experience it is known that such seals on occasions behave as if they were not free, and in that case they act as fixed, unloaded plain cylindrical bearings which is a potential source of instability.

Simulating the oilseals as unloaded cylindrical bearings with a length of 1.25 in., the resulting frequency diagram is shown in Fig. 8. A comparison with Fig. 7 shows that the seals cause a shift in the mode curves, although the change in the first critical speed is small, and, of greater importance, the rotor becomes unstable at 8280 rpm. Therefore, to insure adequate stability margin the destabilizing capability of the seals should be reduced. The simplest method is to cut one or several circumferential grooves in the seal surface, thereby preventing the buildup of the hydrodynamic pressures in the film to become too large.

When it is not possible or feasible to make modifications in those components which are responsible for the instability, the rotor may be stabilized by providing external damping by means of damper bearings. This is illustrated in Fig. 9 which applies to

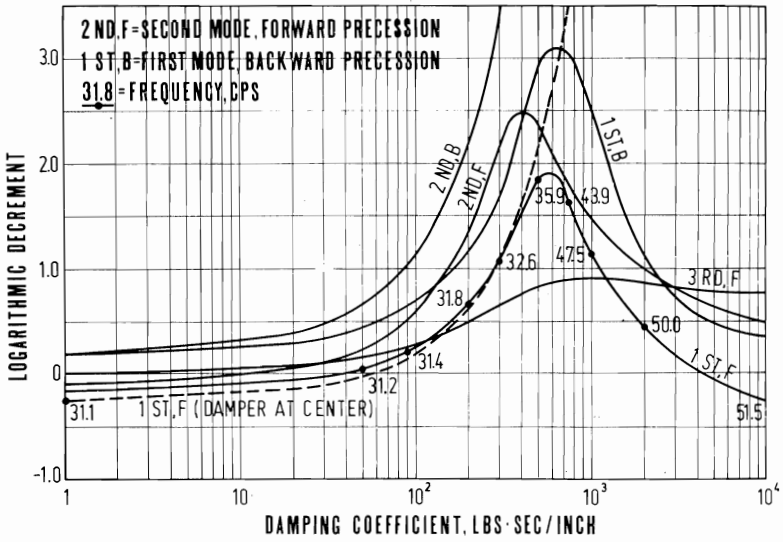

Fig. 9 Stabilization of 8 stage compressor in plain cylindrical journal bearings, mounted in damper bearings with stiffness = 100,000 lb/in. and damping coefficient given by the abscissa; dotted curve applies to damper bearing at rotor center

the compressor rotor supported in plain cylindrical bearings and running at 9000 rpm. The damper bearings are built in between the bearing housings and the pedestals. They have a stiffness of 100,000 lb/in. while the damping coefficient is varied over a range as shown in Fig. 9. The critical mode is the forward precessional mode of the first rotor mode, identified as "1st,F," and it is stable when the damping coefficient is between 40 and 4000 lb·sec/in. The optimum damping value is approximately 600 lb·sec/in. which, at the same time, also improves the damping of the other modes.

Even though the damper bearings could be made somewhat stiffer than the selected value of 100,000 lb/in., they still may be too soft for the application. In that case an alternative method is to provide a damper bearing which acts directly on the shaft. Obviously, the most convenient location would be one of the shaft ends outboard of the bearings, but calculations show the effect to be negligible.

Instead, calculations have been performed with a damper bearing located at the center of the rotor, and the results for the first mode (forward precession) are given by the dotted curve in Fig. 9. The bearing is assigned a nominal stiffness of 500 lb/in. for centering purposes, and its damping coefficient is varied over a range as shown. As can be seen, the bearing is very efficient in stabilizing the rotor but, in practice, it would be difficult to provide a damper bearing at this particular location.

Summary and Conclusions

A method has been developed to calculate the damped natural frequencies (the eigenvalues) of a general flexible rotor supported in fluid-film journal bearings. The rotor model also incorporates internal hysteretic shaft damping and destabilizing aerodynamic forces.

The method is basically an extension of the Myklestad-Prohl method for calculating critical speeds, which utilizes the computational procedure of the well-known Holzer method. As such, the method can readily be applied to a wide variety of rotor and support configurations and is easily programmed for numerical computation. The program is simple with a fast execution time.

The calculated eigenvalues establish the stability margin of the rotor system, conveniently expressed in terms of the logarithmic decrement of the eigenvalue closest to the threshold of instability. If the margin is insufficient, or the rotor even is found to become unstable, the program can be used to explore possible means of improvement, either by reducing or eliminating the sources causing the instability, by design modifications of the shaft or the bearings, or by providing stabilizing external damping through damper bearings. In performing such investigations, and to optimize corrective measures, the program can be a valuable design tool.

The obtained damped natural frequencies also establish the actual critical speeds of the rotor, including the stiffening effect of the damping in the bearings. These results give a more realistic base than the conventional critical speed calculation for assessing any potential trouble from passing through or operating close to a critical speed. In addition, knowing the logarithmic decrement at the critical speeds and, thereby, the response amplification factor, means are provided for evaluating the rotors sensitivity to mass unbalance.

APPENDIX

The eigenvalues for a uniform shaft, supported at the ends in identical bearings which are represented by a single stiffness and a single dashpot, may be determined from impedance matching at the bearings. Ignoring contributions from shear deformation, rotary inertia, and gyroscopic moments, the conventional beam equation is

$$\frac{\partial^2}{\partial z^2}\left(EI\frac{\partial^2 x}{\partial z^2}\right) + \rho A\frac{\partial x^2}{\partial l^2} = \delta(z)\cdot f_0 + \delta(z-l)\cdot f_l \qquad (22)$$

where f_0 and f_l are the bearing reactions and $\delta(z)$ is the delta function.

The solutions to the homogeneous equation are the modal functions, X_n, for a free-free beam. The associated resonant frequencies, ω_n, are the solutions to the transcendental equation

$$\cosh\left(\pi\sqrt{\frac{\omega_n}{\omega_0}}\right)\cdot\cos\left(\pi\sqrt{\frac{\omega_n}{\omega_0}}\right) = 1 \qquad (23)$$

where ω_0 is the lowest resonant frequency of the corresponding rigidly supported beam

$$\omega_0 = \frac{\pi^2}{l^2}\cdot\sqrt{\frac{EI}{\rho A}} \qquad (24)$$

The solutions are

$$\omega_1 = \omega_2 = 0$$

$$\omega_3/\omega_0 = 2.26689$$

$$\omega_4/\omega_0 = 6.24876$$

$$n \geq 5: \quad \omega_n/\omega_0 \geq (n - 3/2)^2$$

The modal functions are orthogonal

$$\int_0^l \rho A\cdot X_n\cdot X_m dz = \begin{cases} 0 & (n \neq m) \\ N_n & (n = m) \end{cases} \qquad (25)$$

N_n is the modal norm

$$N_n = \begin{cases} M\cdot(X_n)_0^2 & (n = 1) \\ \frac{1}{3}M\cdot(X_n)_0^2 & (n = 2) \\ \frac{1}{4}M\cdot(X_n)_0^2 & (n \geq 3) \end{cases} \qquad (26)$$

where $M = \rho A l$ is the total shaft mass and $(X_n)_0$ is the assigned value of X_n at $z = 0$.

The normal coordinates, q_n, are introduced by

$$x = \sum_{k=1}^{\infty} X_k\cdot q_k \qquad (27)$$

Assuming a solution for q_k of exponential form, equation (27) can be substituted into equation (22). Making use of equation (25), the solution becomes

$$q_n = \frac{(X_n)_0 f_0 + (X_n)_l f_l}{N_n(s^2 + \omega_n^2)}\cdot e^{st} \qquad (28)$$

With a bearing stiffness, K, and a damping coefficient, B, the bearing reaction is

$$f_0 = -(K + sB)\cdot x(0) \qquad (29)$$

and analogously for f_l. Because of symmetry, $x(l) = \pm x(0)$ and $(X_n)_l = \pm(X_n)_0$ where the plus sign applies to the even modes (n odd) and the minus sign to the odd modes (n even). Thus, by combining equations (26)–(29), the eigenvalues for the shaft-bearing system, s, are determined from the equation

$$-\frac{l^3}{\pi^4 EI}\cdot(K + sB) = \frac{l^3}{\pi^4 EI}\cdot Z_r = \begin{cases} \frac{1}{2}\cdot\left[\dfrac{1}{\left(\frac{s}{\omega_0}\right)^2} + 4\sum\limits_{n=1,3,-}\dfrac{1}{\left(\frac{s}{\omega_0}\right)^2 + \left(\frac{\omega_n}{\omega_0}\right)^2}\right]^{-1} \\ \frac{1}{2}\cdot\left[\dfrac{3}{\left(\frac{s}{\omega_0}\right)^2} + 4\sum\limits_{n=2,4,-}\dfrac{1}{\left(\frac{s}{\omega_0}\right)^2 + \left(\frac{\omega_n}{\omega_0}\right)^2}\right]^{-1} \end{cases} \qquad (30)$$

Z_r is the shaft impedance, defined through this equation. The equation may be solved numerically. Typical results are shown in Figs. 1 and 2 where $\pi^4 EI/l^3 = 2.9378\cdot 10^5$ and K is equal to 20,000 and 60,000 lb/in., respectively.

With s real, it is found from equation (30) that there can exist at most two pairs of real roots, one pair for the even modes and one pair for the odd modes. Hence, a maximum of two modes will be critically damped. When the bearings are of the fluid-film type they cannot, in general, be represented by a single stiffness and a single damping coefficient. Instead of just one impedance, four impedances are required

$$Z_{xx} = K_{xx} + sB_{xx} \tag{31}$$

and similarly for Z_{xy}, Z_{yx}, and Z_{yy} where the first index gives the direction of the reaction force and the second index gives the amplitude direction. By matching impedances at the bearings, the eigenvalues are determined from the determinantal equation

$$\begin{vmatrix} (Z_{xx} + Z_r) & Z_{xy} \\ Z_{yx} & (Z_{yy} + Z_r) \end{vmatrix} = 0 \tag{32}$$

where the shaft impedance, Z_r, is given by equation (30). The solution becomes

$$-Z_r = \frac{1}{2}(Z_{xx} + Z_{yy}) \pm \sqrt{\frac{1}{4}(Z_{xx} - Z_{yy})^2 + Z_{xy}Z_{yx}} \tag{33}$$

Whereas the one-dimensional bearing in equation (30) only yields one eigenvalue per shaft mode, there are two eigenvalues with the two-dimensional fluid-film bearing (an eigenvalue is considered to consist of a pair of roots). Corresponding to the two eigenvalues, each mode has a forward precessional component and a backward precessional component. As in the previous case, equation (33) shows that there are, at most, two pairs of real roots. Thus a maximum of two mode components can be critically damped, one even and one odd mode component.

Typical results are shown in Fig. 3 where the shaft is the same as considered in Figs. 1 and 2 but the bearings are of the plain cylindrical type with dimensions as given in the discussion.

References

1 Prohl, M. A., "A General Method for Calculating Critical Speeds of Flexible Rotors," *Journal of Applied Mechanics*, Vol. 12, TRANS. ASME, Vol. 67, 1945, pp. A-142–A-148.

2 Myklestad, N. O., "A New Method of Calculating Natural Modes of Uncoupled Bending Vibration of Airplane Wings and other Types of Beams," *Journal of the Aeronautical Sciences*, Apr. 1944, pp. 153–162.

3 Timoshenko, S., *Vibration Problems in Engineering*, D. Van Nostrand Company, Inc., 1959.

4 Dimentberg, F. M., *Flexural Vibrations of Rotating Shafts*, Butterworths, London, 1961.

5 Gladwell, G. M. L., and Bishop, R. E. D., "The Vibration of Rotating Shafts Supported in Flexible Bearings," *Journal of Mechanical Engineering Science*, Vol. 1, No. 3, 1959, pp. 195–206.

6 Pedersen, P. T., "Rotors With Unsymmetrical Flexible Bearings," dissertation, Department of Applied Mechanics, Technical University of Denmark, May 1969.

7 Tang, T. M., and Trumpler, P. R., "Dynamic of Synchronous-Precessing Turborotors With Particular Reference to Balancing, Part I—Theoretical Foundations," *Journal of Applied Mechanics*, Vol. 31, TRANS. ASME, Vol. 86, Series E, Mar. 1964, pp. 115–122.

8 Lund, J. W., and Orcutt, F. K., "Calculations and Experiments on the Unbalance Response of a Flexible Rotor," JOURNAL OF ENGINEERING FOR INDUSTRY, TRANS. ASME, Series B, Vol. 89, No. 4, Nov. 1967, pp. 785–796.

9 Gunter, E. J., "Dynamic Stability of Rotor-Bearing Systems," "NASA SP-113, Office of Technology Utilization, U. S. Government Printing Office, 1966.

10 Suter, P., "Lagernachgiebigkeit und -dämpfung bei der Ersten Kritischen Drehzahl," *Technische Rundschau Sulzer*, Vol. 3, 1962, pp. 38–44.

11 Krämer, E., "Der Einfluss des Ölfilms von Gleitlagern auf die Schwingungen von Maschinenwellen," *VDI-Berichte*, Vol. 35, 1959, pp. 135–145.

12 Ono, K., and Tamura, A., "On the Vibrations of Horizontal Shaft Supported in Oil-Lubricated Journal Bearings," Bulletin of *Japan Society of Mechanical Engineers*, Vol. 11, No. 47, 1968, pp. 813–824.

13 Holmes, R., "The Vibration of a Rigid Shaft on Short Sleeve Bearings," *Journal of Mechanical Engineering Science*, Vol. 2, No. 2, 1960, p. 337.

14 Lund, J., "Rotor-Bearing Dynamics Design Technology, Part VII: The Three Lobe Bearing and Floating Ring Bearing," Report No. AFAPL-TR-65-45, Part VII, Wright-Patterson Air Force Base, Ohio, Feb. 1968.

15 Lund, J. W., "Spring and Damping Coefficients For the Tilting Pad Journal Bearing," *Transactions of the ASLE*, Vol. 7, 1964, pp. 342–352.

16 Krämer, E., "Feder-und Dämpfungszahlen von Gleitlagern," VDI-Berichte, No. 135, 1969, pp. 117–123.

17 Pestel, E., "Beitrag zur Ermittlung der hydrodynamischen Dämpfungs-und Federeigenschaften von Gleitlagern," *Ingenieur-Archiv*, Vol. 22, No. 3, 1954, pp. 147–155.

18 Smith, D. M., *Journal Bearings in Turbomachinery*, Chapman and Hall Ltd., 1969.

19 Glienicke, J., "Feder-und Dämpfungskonstanten von Gleitlagern für Turbomaschinen und deren Einfluss auf das Schwingungsverhalten eines einfachen Rotors," dissertation, Technische Hochschule Karlsruhe, 1966.

20 Glienicke, J., "Experimental Investigation of the Stiffness and Damping Coefficients of Turbine Bearings and Their Application to Instability Prediction," *Journal Bearings for Reciprocating and Turbo Machinery*, Symposium in Nottingham, Sept. 1966, pp. 122–135.

21 Mitchell, J. R., Holmes, R., and van Ballegooyen, H., "Experimental Determination of a Bearing Oil-Film Stiffness," *Proceedings, Institution of Mechanical Engineers*, Vol. 180, Part 3K, 1965–1966, Paper No. 2, pp. 90–96.

22 Glienicke, J., "Schwingungs-und Stabilitätsuntersuchungen an gleitgelagerten Rotoren," *Motortechnische Zeitschrift*, Vol. 33, No. 4, Apr. 1972, pp. 135–139.

23 Someya, T., "Stabilität einer in zylindrischen Gleitlagern laufenden, unwuchtfreien Welle," dissertation, Technische Hochschule Karlsruhe, 1962.

24 De Choudhury, P., and Gunter, E. J., "Dynamic Stability of Flexible Rotor-Bearing Systems," Report No. ME-4040-104-70U, University of Virginia, Charlottesville, Dec. 1970.

25 Alford, J. S., "Protecting Turbomachinery From Self-Excited Rotor Whirl," *Journal of Engineering for Power*, TRANS. ASME, Series A, Vol. 87, Oct. 1965, pp. 333–344.

26 Pollmann, E., "Stabilität einer in Gleitlagern rotierenden Welle mit Spalterregung," *Fortschritt Berichte, VDI-Z*, Series 1, No. 15, May 1969.

27 Winter, C. J., "Lastabhängige instabile Bewegungen von Turbinenläufern," dissertation, Technische Hochschule Darmstadt, 1968.

28 Gasch, R., "Selbsterregte Biegeschwingungen rotierender Wellen," *Konstruktion*, Vol. 23, No. 1, 1971, pp. 5–13.

29 Ehrich, F. F., "Shaft Whirl Induced by Rotor Internal Damping," *Journal of Applied Mechanics*, Paper no. 64-APM-7.

30 Myklestad, N. O., "The Concept of Complex Damping," *Journal of Applied Mechanics*, Sept. 1956.

31 Brown, P. F., "Bearings and Dampers for Advanced Jet Engines," Society of Automotive Engineers, Paper No. 700318, National Air Transportation Meeting, New York, N. Y., Apr. 1970.

32 Ruhl, R. L., and Booker, J. F., "A Finite Element Model for Distributed Parameter Turborotor Systems," JOURNAL OF ENGINEERING FOR INDUSTRY, TRANS. ASME, Series B, Vol. 94, No. 1, Feb. 1972, pp. 126–132.

Printed in U. S. A.